

**Test of the Skyrme Effective Field Theory
Using Quenched Lattice QCD***

M.-C. Chu[†]

*Center for Theoretical Physics, Laboratory for Nuclear Science
and Department of Physics, Massachusetts Institute of Technology
Cambridge, Massachusetts 02139 U.S.A.*

Marcello Lissia

*Istituto Nazionale di Fisica Nucleare
Sezione di Cagliari
Via Ada Negri 18, I-09127 Cagliari, ITALY*

and

J. W. Negele

*Center for Theoretical Physics, Laboratory for Nuclear Science
and Department of Physics, Massachusetts Institute of Technology
Cambridge, Massachusetts 02139 U.S.A.*

ABSTRACT

The Skyrme effective field theory is tested by evaluating nucleon ground state matrix elements of the correlation functions for two flavor density operators and two pseudoscalar density operators in the Skyrme model and comparing them with results in quenched lattice QCD. The possibility of using quenched lattice QCD to study higher-order terms in effective field theory is also discussed.

Submitted to: *Nuclear Physics A*

CTP#2004

hep-lat/9308012

July 1993

* This work is supported in part by funds provided by the U. S. Department of Energy (D.O.E.) under contract #DE-AC02-76ER03069.

[†] Current address: W. K. Kellogg Radiation Laboratory, Caltech 106-38, Pasadena CA 91125, U.S.A.

I. INTRODUCTION

The Skyrme model⁽¹⁻⁴⁾ provides an appealing but incomplete step towards the goal of constructing a systematic, quantitative effective field theory for baryons. In the large N limit, QCD becomes equivalent to an effective theory of mesons, and baryons emerge naturally as solitons of this theory. The simplest Lagrangian for the effective theory, obtained by Skyrme by adding a non-minimal term to the non-linear sigma model to stabilize these solitons¹, provides a remarkably successful schematic model of the nucleon. However, despite the large body of research studying specific corrections and extensions since Adkins, Nappi and Witten² revived interest in the Skyrme model a decade ago by proposing it as a serious model of the nucleon, the effective field theory has never been developed and tested in a controlled way.

Hence, the motivation for this present work is to use quenched lattice QCD as a framework for the controlled and systematic study of effective field theory. In contrast to studies of physical hadrons, for which the omission of fermion loops in quenched QCD represents an uncontrolled approximation, the fact that fermion loops are negligible in the large N limit implies that there is a meaningful effective meson theory for quenched QCD. Hence, lattice solutions of quenched QCD provide an ideal laboratory to systematically test every aspect of the approximations introduced in effective field theory. Relative to comparisons with experiment, the lattice QCD laboratory provides the opportunity both to explore the approximations as a function of fundamental parameters, such as the quark mass, and to study quantities which are not readily amenable to experiment, such as two-body correlation functions. Since quenched lattice QCD reproduces masses and hadron properties which are close to experiment for the physical quark masses, we expect the conclusions concerning effective field theory to be relevant to physical hadrons.

To clarify the aspects of the effective field theory formulation we would ultimately like to explore, it is useful to consider the functional integral for full QCD. Meson fields may be introduced by writing delta-functions setting each meson field equal to appropriate bilinear quark fields and integrating over the meson fields. The relevant effective action is then defined by the functional integral over quark and gluon fields with the delta-function constraints, and this action is to be integrated over all the meson fields, corresponding to the calculation of all quantum loop corrections to the stationary-phase approximation. Similarly, effective operators are defined by the ratio of the functional integral over quark and gluon fields of the action multiplied by the original quark and gluon operator and delta-function constraints divided by the corresponding integral without the operator. In this framework, one could systematically study the effects of truncating to various numbers of meson fields, of truncating the terms in a derivative expansion of the effective action, of truncating at various levels in the loop expansion of quantum corrections, and of retaining various terms in the expressions for effective operators. In this language, the simplest version of the Skyrme model is obtained by retaining only the pion field, arguing by symmetry and simplicity that only the non-linear sigma model kinetic energy and Skyrme terms need be retained in the action, assuming that N is large enough that quantum corrections to the properly projected degenerate classical solutions may be neglected, and arguing that the relevant effective operators are uniquely specified by symmetry considerations. In principle, each of the four classes of approximation

may be tested quantitatively by lattice calculations, affording the opportunity to explore systematically all of the approximations underlying the effective theory.

In this present work, we take the first step in such a program by comparing correlation functions in the nucleon calculated on the lattice with corresponding correlation functions calculated in the simplest version of the Skyrme model. For each value of the quark mass, we take the the lattice observables as defining a model system, which we approximate by an effective Skyrme Lagrangian. As in the work of Adkins and Nappi³, we use the values of the pion, nucleon, and delta masses to specify the three parameters in the Skyrme Lagrangian, which then predict all other observables. Since we wish to study the validity of the effective theory for hadron structure, we focus our attention on two correlation functions we have calculated previously which explore the spatial distribution of the nucleon: the density-density correlation function and the pseudoscalar correlation function. Naively, since the original Skyrme model with parameters determined from hadron masses³ makes a 40% error in F_π , we expect errors up to this order of magnitude in other observables. In addition we expect the effective theory to improve as the pion becomes lighter. To the extent to which these expectations are borne out and the effective theory provides a reasonable first approximation to the lattice results, we believe we have established a useful framework for quantitative investigation of each of the corrections discussed above.

The outline of this paper is as follows. In section II, we describe the operators and correlation functions which are evaluated on the lattice and our identification of corresponding operators in the Skyrme model. Using the standard spin-isospin projected hedgehog solution, analytic expressions for the correlation functions are presented and the details of the derivations are given in the Appendix. The results for the density-density and pseudoscalar correlation functions in the Skyrme model are compared with corresponding lattice results in section III and the conclusions are discussed in the last section.

II. Operators and Correlation Functions in Lattice QCD and in the Skyrme Model

Since the QCD and the Skyrme Lagrangians are defined in terms of different degrees of freedom, in the absence of a systematic derivation of effective operators as discussed in the introduction, the determination of the operators in the Skyrme model to be compared with lattice operators might appear ambiguous. However, at the level of truncation considered here, we will show that the appropriate operators may be determined from symmetry considerations.

The Skyrme Lagrangian has been constructed such that it shares those QCD symmetries believed to be relevant to low-energy phenomenology: the $SU(2)_L \otimes SU(2)_R$ flavor symmetry, with its $SU(2)_V$ subgroup that corresponds to isospin conservation, and a topologically conserved current that corresponds to baryon number conservation. Since each operator of interest to us in QCD is induced by a symmetry operation on the QCD Lagrangian, we define the corresponding operator in the effective theory as the operator induced by the same symmetry operation on the Skyrme Lagrangian.

density operators

The two flavor density operators we measure in lattice QCD are $\hat{\rho}_u(\vec{r}) \equiv: \bar{u}(\vec{r})\gamma^0 u(\vec{r}):$ and $\hat{\rho}_d(\vec{r}) \equiv: \bar{d}(\vec{r})\gamma^0 d(\vec{r}):$. These operators may be written as linear combinations of the

time-components of the conserved baryon current B^μ and conserved isospin current $V^{\mu,a}$ ($a = 1, 2, 3$), which correspond in the standard way to the isoscalar and isospin symmetries of QCD:

$$\hat{\rho}_d^u(\vec{r}) = \frac{3}{2}\hat{B}^0(\vec{r}) \pm \frac{1}{2}\hat{V}^{0,3}(\vec{r}) \quad . \quad (2.1)$$

Our normalization conventions are such that $\int d^3r \hat{V}^{0,a}(\vec{r}) = 2I_a$ (a^{th} component of the isospin operator), $\int d^3r \hat{B}^0(\vec{r}) = \hat{B}$ (baryon number operator) and $\int d^3r \hat{\rho}_{u,d} = \hat{N}_{u,d}$ (flavor number operator). Since isospin is unbroken in QCD with equal quark masses and in the Skyrme model, both currents are exactly conserved. Hence they do not get renormalized and the normalization in Eq. (2.1) has an absolute meaning. Although it is possible to write conserved currents on the lattice, the local currents we have used are not conserved and have normalization factors which differ from unity by the order of 10%. As will be shown subsequently, this is not a problem in practice since the isoscalar current strongly dominates the isovector current. Therefore a 10% error in the relative normalization is negligible and the overall density is normalized such that it integrates to unity.

We then may write the correlation between the up and down quark density as

$$\begin{aligned} \langle \hat{\rho}_u(\vec{r})\hat{\rho}_d(\vec{r}') \rangle &= \frac{9}{4} \langle \hat{B}^0(\vec{r})\hat{B}^0(\vec{r}') \rangle - \frac{1}{4} \langle \hat{V}^{0,3}(\vec{r})\hat{V}^{0,3}(\vec{r}') \rangle \\ &\stackrel{\text{class.}}{\equiv} \frac{9}{4} \langle \hat{B}^0(\vec{r}) \rangle \langle \hat{B}^0(\vec{r}') \rangle - \frac{1}{4} \langle \hat{V}^{0,3}(\vec{r}) \rangle \langle \hat{V}^{0,3}(\vec{r}') \rangle \\ &\equiv \frac{9}{4} B^0(\vec{r})B^0(\vec{r}') - \frac{1}{4} V^{0,3}(\vec{r})V^{0,3}(\vec{r}') \quad . \end{aligned} \quad (2.2)$$

While the first equality is valid in general, the second one is only valid if we consider the classical solution and disregard the quantum fluctuations⁵. This is the approximation in which we solve the Skyrme model.

We therefore compare the density-density correlation function evaluated in the nucleon ground state on the lattice

$$\langle \rho_0 \rho_0 \rangle_L(y) \equiv \int \frac{d^3r d^3r' \delta(y - |\vec{r} - \vec{r}'|)}{4\pi y^2} \langle \hat{\rho}_u(\vec{r})\hat{\rho}_d(\vec{r}') \rangle \quad , \quad (2.3)$$

with the following function calculated in the Skyrme model

$$\begin{aligned} \langle \rho_0 \rho_0 \rangle_S(y) &\equiv \frac{9}{4} \int \frac{d^3r d^3r' \delta(y - |\vec{r} - \vec{r}'|)}{4\pi y^2} B^0(\vec{r})B^0(\vec{r}') \\ &\quad - \frac{1}{4} \int \frac{d^3r d^3r' \delta(y - |\vec{r} - \vec{r}'|)}{4\pi y^2} V^{0,3}(\vec{r})V^{0,3}(\vec{r}') \quad . \end{aligned} \quad (2.4)$$

Here $B^\mu(\vec{r})$ and $V^{\mu,3}(\vec{r})$ are the standard currents of the Skyrme Lagrangian: $B^\mu(\vec{r})$ is the topological baryon current⁶, and $V^{\mu,a}$ are the Noether currents corresponding to isospin symmetry. These currents are evaluated for the hedgehog solution and normalized such that

$\int d^3r B^0(\vec{r}) = 1$ and $\int d^3r V^{0,3}(\vec{r}) = 2I_3$. The explicit forms of these currents, using the hedgehog solution to the classical equation of motion, $U(\vec{r}) = e^{i\hat{r}\cdot\vec{\tau}F(\tilde{r})}$, are:

$$B^0(\vec{r}) = -\frac{(eF_\pi)^3}{2\pi^2} \frac{\sin^2 F(\tilde{r})}{\tilde{r}^2} \frac{dF(\tilde{r})}{d\tilde{r}} \quad (2.5)$$

$$V^{0,a}(\vec{r}) = F_\pi^2 \frac{\Lambda(\tilde{r})}{\lambda} \left\{ 2I_a - \left[3\vec{I} \cdot \hat{r}_R \hat{r}_R - I_a \right] \right\} , \quad (2.6a)$$

$$\Lambda(\tilde{r}) \equiv \frac{1}{6} \sin^2 F(\tilde{r}) \left\{ 1 + 4 \left[\left(\frac{dF(\tilde{r})}{d\tilde{r}} \right)^2 + \frac{\sin^2 F(\tilde{r})}{\tilde{r}^2} \right] \right\} , \quad (2.6b)$$

$$\lambda \equiv \frac{1}{e^3 F_\pi} \int d^3\tilde{r} \Lambda(\tilde{r}) = \frac{1}{e^3 F_\pi} \tilde{\lambda} . \quad (2.6c)$$

The definition of λ agrees with Ref. [2] and for convenience we have defined the dimensionless constants $\tilde{\lambda}$ and $\tilde{r} = eF_\pi r$. The vector \hat{r}_R is the unit vector in the \vec{r} direction rotated by a time-dependent angle, where this rotation is introduced to project the hedgehog onto states of definite spin and isospin. Since we integrate functions that depend only on the relative direction between \hat{r} and \hat{r}' over the angles $d\Omega(\hat{r})$ and $d\Omega(\hat{r}')$, we can always rotate back to \hat{r}, \hat{r}' and we never need to know the rotation explicitly. Details on how these currents and $F(\tilde{r})$ are derived are given in the Appendix. As mentioned previously, lattice measurements of the pion, nucleon and delta masses are used to determine the numerical values of the three parameters that enter in the equation for $F(\tilde{r})$: the pion mass m_π , the pion decay constant F_π and rho-pion coupling constant e .

As shown in the Appendix, the final formula we obtain for nucleon states, once angular integration has been performed is:

$$\begin{aligned} \frac{1}{(eF_\pi)^3} \langle \rho_0 \rho_0 \rangle_{\text{Skyrme}}(\tilde{y}) &= \frac{9}{4\pi^3} \frac{1}{\tilde{y}} \int_{\frac{1}{2}\tilde{y}}^{\infty} d\tilde{r} \frac{\sin^2 F(\tilde{r})}{\tilde{r}} \frac{dF(\tilde{r})}{d\tilde{r}} \int_{|\tilde{y}-\tilde{r}|}^{\tilde{r}} d\tilde{r}' \frac{\sin^2 F(\tilde{r}')}{\tilde{r}'} \frac{dF(\tilde{r}')}{d\tilde{r}'} \\ &- \frac{3\pi}{4\tilde{\lambda}^2} \frac{1}{\tilde{y}} \int_{\frac{1}{2}\tilde{y}}^{\tilde{r}} d\tilde{r} \tilde{r} \Lambda(\tilde{r}) \int_{|\tilde{y}-\tilde{r}|}^{\tilde{r}} d\tilde{r}' \tilde{r}' \Lambda(\tilde{r}') \left[1 + \left(\frac{\tilde{r}^2 + \tilde{r}'^2 - \tilde{y}^2}{2\tilde{r}\tilde{r}'} \right)^2 \right] \end{aligned} \quad (2.7)$$

where $\tilde{y} = eF_\pi y$ and we used $(I_3)^2 = \frac{1}{4}$ for nucleon states.

Pseudoscalar Operators

The other operators we measured on the lattice are the pseudoscalar density operators $\hat{\rho}_u^5(\vec{r}) \equiv \bar{u}(\vec{r})\gamma^5 u(\vec{r})$ and $\hat{\rho}_d^5(\vec{r}) \equiv \bar{d}(\vec{r})\gamma^5 d(\vec{r})$. For establishing the correspondence between operators in QCD and in the Skyrme model, it is useful to note that these operators are proportional to global chiral variations of the QCD Lagrangian containing a mass term that explicitly breaks the symmetry. For notational simplicity, for a chiral transformation $\psi \rightarrow e^{i\chi\gamma^5}\psi$ we will denote the chiral variation $\frac{\delta}{\delta\chi}$ by δ_C . Then, disregarding for a moment the flavor content, a chiral variation of the QCD Lagrangian yields $\delta_C \mathcal{L}_{\text{QCD}} \sim 2m_q \bar{\psi}\gamma^5\psi$. Using the fact that the ratio m_q/m_π^2 is finite in the chiral limit (proportional to $F_\pi^2 / \langle \bar{\psi}\psi \rangle$), an

equivalent form for $\hat{\rho}^5(r)$ written purely in terms of the Lagrangian and pion mass which has a well defined chiral limit is:

$$\hat{\rho}^5(r) = \frac{m_\pi^2}{2m_q} \frac{\delta_C \mathcal{L}}{m_\pi^2} \propto \frac{\delta_C \mathcal{L}}{m_\pi^2} \quad (2.8)$$

As for the flavor densities, we may write the chiral variation as a linear combination of isoscalar and isovector terms. If we denote the variation of the QCD Lagrangian under an isoscalar chiral rotation by $\delta_{CS} \mathcal{L}_{\text{QCD}}$ and the variation under an isovector chiral rotation by $\delta_{CV} \mathcal{L}_{\text{QCD}}$ we may write:

$$\hat{\rho}_{u,d}^5 = a_{u,d} m_\pi^{-2} \delta_{CS} \mathcal{L}_{\text{QCD}} + b_{u,d} m_\pi^{-2} \delta_{CV} \mathcal{L}_{\text{QCD}} \sim a_{u,d} m_\pi^{-2} \partial_\mu \hat{S}_5^\mu + b_{u,d} m_\pi^{-2} \partial_\mu \hat{V}_5^{\mu,3} \quad , \quad (2.9)$$

where S_5^μ and $V_5^{\mu,a}$ ($a = 1, 2, 3$) are the corresponding Noether currents which are conserved in the chiral limit, and the a 's and b 's are known constants which are finite in the chiral limit. We may then define the analogous operators in the Skyrme model to within the ambiguity of the choice of the mass term, for which we make the standard choice of $\mathcal{L}' = \frac{1}{8} m_\pi^2 F_\pi^2 (\text{Tr} U - 2)$. Since the two operators on the right-hand side of Eq. (2.9) are not conserved, in general one would have to calculate the renormalized operators to determine the correct linear combination. However, for the Skyrme Lagrangian $\delta_{CS} \mathcal{L}_{\text{Skyrme}} = 0$ by definition. That is, the variation is outside the $SU(2)$ manifold where the theory is defined and there is no anomalous contribution as for the baryon number. Hence, in the Skyrme model both flavor operators have only the isovector contribution

$$[\hat{\rho}_u^5(\vec{r})]_{\text{Skyrme}} \sim [\hat{\rho}_d^5(\vec{r})]_{\text{Skyrme}} \sim m_\pi^{-2} \delta_{CV} \mathcal{L}_{\text{Skyrme}} \sim m_\pi^{-2} \partial_\mu V_5^{\mu,3} \quad . \quad (2.10)$$

Physically, this result corresponds to the fact that the the Skyrme model describes the $\rho_u^5 - \rho_d^5$ correlation as a pion-pion correlation, and from PCAC we recognize $m_\pi^{-2} \partial_\mu V_5^{\mu,3}$ as a pion interpolating field. There is no contribution from pseudo-scalar isoscalar particles since the η and η' are not included in the model. One might argue whether the model makes a good approximation in keeping only the light pion degrees of freedom, but once we are given this model Lagrangian, the comparison with QCD is unambiguous. We clearly expect this approximation to improve as we lower the pion mass.

Only the mass term $\mathcal{L}' = \frac{1}{8} m_\pi^2 F_\pi^2 (\text{Tr} U - 2)$ in the Skyrme Lagrangian contributes to the chiral variation $\delta_{CV} \mathcal{L}_{\text{Skyrme}}$:

$$m_\pi^{-2} \delta_{CV} \mathcal{L}' = -\frac{1}{4} F_\pi^2 \text{Tr} (iU \tau_3) = \frac{1}{2} F_\pi^2 \sin F(\tilde{r}) \hat{r}_R \cdot \hat{z} \quad (2.11a)$$

where again \hat{r}_R is the rotated vector and, once we change variables from \hat{r} to \hat{r}_R , we obtain

$$\rho_u(\vec{r}) \sim \rho_d(\vec{r}) \sim F_\pi^2 \sin F(\tilde{r}) \cos \theta \quad . \quad (2.11b)$$

Note that the operator has a well defined chiral limit in the Skyrme model. Hence, finally we compare the correlation function evaluated in the nucleon ground state on the lattice

$$\langle \rho_5 \rho_5 \rangle_L(y) \sim \int \frac{d^3 r d^3 r' \delta(y - |\vec{r} - \vec{r}'|)}{4\pi y^2} \langle \hat{\rho}_u^5(\vec{r}) \hat{\rho}_d^5(\vec{r}') \rangle \quad , \quad (2.12)$$

with the following Skyrme model correlation function:

$$\begin{aligned}
\langle \rho_5 \rho_5 \rangle_S(y) &\sim \int \frac{d^3 r d^3 r' \delta(y - |\vec{r} - \vec{r}'|)}{4\pi y^2} \sin F(\tilde{r}) \sin F(\tilde{r}') \cos \theta \cos \theta' \\
&\sim \frac{1}{y} \int_{\frac{1}{2}y}^{\infty} dr \sin F(\tilde{r}) \int_{|y-r|}^r dr' \sin F(\tilde{r}') [r^2 + r'^2 - y^2] \quad .
\end{aligned} \tag{2.13}$$

The overall normalization cannot be defined unambiguously as explained before, and we can only compare the shapes of the two functions. Details of the angular integration are given in the Appendix.

To explore the ambiguity in the pseudoscalar current induced by the choice of the mass term, we have considered two alternatives to the standard result in Eq. (2.11) and compare the resulting correlation functions in Figure 1. Since we make the comparisons in the chiral limit, $m_\pi = 0$, it is clear that each of the currents is consistent with the Lagrangian and simply corresponds to a different arbitrary choice of non-linear terms in the pion field. The standard result from Eq. (2.11) is shown by the solid curve and labeled by $\sin(F)$. Variation of the mass term $\mathcal{L}' = \frac{1}{32} m_\pi^2 F_\pi^2 (\text{Tr } U^2 - 2)$ yields a pseudoscalar density proportional to $\frac{1}{2} \sin(2F)$ and the resulting correlation function is shown by the dot-dashed line. In general, any term or combination of terms of the form $\mathcal{L}'_k = \frac{1}{8k^2} m_\pi^2 F_\pi^2 \text{Tr}(U^k - 1)$ gives the expected asymptotic pion mass term and provides a possible alternative. The curve labeled by F is obtained by replacing $\sin F(\tilde{r})$ in Eq. (2.11) by its asymptotic form at large \tilde{r} , $F(\tilde{r})$. Note that this result may be viewed as being generated by the Lagrangian term $\mathcal{L}' = \sum_{k=1}^{\infty} (-1)^k \mathcal{L}'_k$. This simple comparison shows explicitly that we can get very different results for correlation functions at short and medium range for different choices of effective operators which are equivalent at large distance. This clearly motivates future efforts to derive or calculate on the lattice higher-order terms in the expansion of effective operators.

In a previous comparison⁷ of the lattice results and the bag model, it was natural to equate the quark field operators of the two theories. In the present context, one may ask whether the results would have been different if we had used operators induced by symmetries. It is readily seen that whereas we would have obtained the same flavor density operators, the pseudoscalar density operators would have been somewhat different. The main point is that in contrast to the QCD and Skyrme Lagrangians, the bag Lagrangian in the basic form used in ref. [7] is not invariant under chiral rotation, even in the limit of zero quark mass. In the chiral limit, the chiral variation receives non-vanishing contributions from the bag surface. This contribution is equal in form to the QCD term, but it is multiplied by a delta function at the surface. Hence, in addition to the double volume integral of the relevant quark wave functions, we would also have had a double surface integral with a weight that would have become dominant in the chiral limit. The shape of this latter contribution is significantly different, even though it retains some of the correct global features such as having zero volume integral⁷.

III. RESULTS

We use quenched lattice QCD calculations at three different values of the bare quark mass to define three test systems which may then be approximated by the Skyrme model. The lattice calculations are carried out on a $16^3 \times 24$ lattice at $\beta = 5.7$ using bag model sources and are described in detail in Refs. [7-10]. We have chosen to define the energy scale of the lattice calculations using the string tension, which gives an inverse lattice spacing $a^{-1} = 1\text{GeV}$ and $a = 0.2\text{fm}$. Although defining the scale using the extrapolated proton mass yields a value of a 15% smaller, the quantitative comparison with the Skyrme model is unaffected since when the Skyrme parameters are determined from the lattice masses, the correlation functions scale in a .

The equation for the soliton, Eq. (A.5), depends only on the dimensionless parameter $\beta = \frac{m_\pi}{eF_\pi}$ and its solution is a function of the dimensionless variable $\tilde{r} = eF_\pi r$. Therefore, the correlation functions we calculate depend only on two parameters, m_π and the scale factor $(eF_\pi)^{-1}$. However, since we link the choice of eF_π to the proton and delta masses through Eq. (A.3), we actually determine e and F_π separately. The four sets of Skyrme parameters we use are shown in Table I, where the masses in bold face have been used as input and the other parameters are predicted by the model. Since the nucleon and delta energies depend nonlinearly on $\frac{m_\pi}{eF_\pi}$, the parameters are determined numerically. A rough idea of the sensitivity of the nucleon or delta mass to eF_π is given by the fact that at $m_\pi = 0$, $\frac{\delta M}{M} \sim 2 \frac{\delta(eF_\pi)}{eF_\pi}$

density-density correlation function

As a prelude to considering the Skyrme model density-density correlation function's dependence on the quark mass and how it compares with the lattice results, it is useful to note the extent to which it is dominated by the isoscalar baryon number density contribution. The isovector and isoscalar contributions, as well as the weighted average $\frac{9}{8} \langle \rho\rho \rangle_S - \frac{1}{8} \langle \rho\rho \rangle_V$ are shown in Figure 2 for the range of pion masses we consider. In all cases, over the spatial range shown in the figure relevant to this work, one observes that the isoscalar and isovector contributions are sufficiently similar that $\frac{1}{8}$ of their difference is very small compared to the isoscalar contribution and the full correlation function is very well approximated by the isoscalar correlation function. This result has two important implications. We may regard the physics as being dominated by the topological baryon number density and, as claimed earlier, we are justified in neglecting differences in the renormalization factors for the isovector and isoscalar density operators on the lattice. The only place the isovector and isoscalar correlation functions differ significantly is in the extreme surface, where the isoscalar correlation decays asymptotically as $e^{-3m_\pi r}$, whereas the isovector correlation function decays as $e^{-2m_\pi r}$. This behavior reflects the leading contributions of two or three pions respectively in each channel and gives rise to the fact that at very large distances, the correlation function changes sign. Similarly, we also expect the correlation to be negative at sufficiently large distance on the lattice.

The change in the shape and spatial extent of the correlation function with quark mass is shown in Figure 3. For convenience, throughout this section we will refer to pion mass dependence interchangeably with quark mass dependence. It is implicit that when we consider

a change in the pion mass, we also consider the correlated changes in F_π and e induced when a change in the bare quark mass produces this change in the pion mass.

A striking feature of Fig. 3 is the fact that the mass dependence is highly non-linear. Indeed, the change in the correlation function caused by reducing m_π by 173 MeV from 515 to 342 MeV is quite small compared to the change caused by reducing m_π by another 205 MeV to 137 MeV. A related indication of how far these masses are from the chiral limit is given by the values shown in Table I for the parameter $\beta = \frac{m_\pi}{e F_\pi}$ governing the hedgehog solution.

The radial extent of the correlation function depends both on the scale factor $(eF_\pi)^{-1}$, which decreases as m_π decreases, and on the exponential tail, which grows as m_π decreases. These two effects go in opposite directions for the cases we consider. It turns out that the scale factor dominates and the net result is shrinking of both the isoscalar and isovector contributions with decreasing m_π . This shrinkage with decreasing m_π is shown both by the increase of the normalized correlation function at zero separation and by the decrease in isoscalar and isovector r.m.s. radii in Table I. (Note that for values of m_π lighter than the physical mass, the isovector radius begins to increase and ultimately diverges in the chiral limit because of chiral logs.) The trend is opposite in the lattice results, where the normalized correlation function at zero separation clearly decreases with m_π . The second moments of the lattice results have sufficiently large errors because of the r^2 weighting of the poorly determined tails that their trend with m_π is not statistically determined. Also note that these second moments of correlation functions are not rms radii of density distributions because of the presence of polarization contributions¹¹.

Lattice measurements of the density-density correlation function for each of the three values of the bare quark mass are compared with the corresponding Skyrme model correlation functions in Figure 4. Because statistical errors in the correlation functions at large radius induce significant errors in the overall normalization, we have normalized all correlation functions to unity at the origin to facilitate comparison. One observes that as the quark mass and thus the pion mass decreases, the agreement improves substantially. Since we are using sufficiently large quark masses that we should not expect the Skyrme model to be an accurate approximation, it is encouraging that the agreement improves so conspicuously as the quark mass decreases. It will therefore be of interest to carry out more detailed comparisons for lighter quark masses, to verify that this agreement is maintained as the correlation function undergoes the significant changes shown in Fig. 3.

pseudoscalar correlation function

In contrast to the density-density correlation function, where both isoscalar and isovector terms contribute, the Skyrme model has only an isovector contribution to the pseudoscalar correlation function. This correlation function decays exponentially in the pion mass at large r and, on physical grounds, it should be the dominant contribution in the chiral limit at large distance. In contrast, the lattice calculation has contributions from both the isoscalar and isovector terms. At the large quark masses we consider in this work, the isovector π and the isoscalar η have comparable masses and may be expected to yield comparable contributions with an overall coefficient that favors the isoscalar one. Hence, we expect the best agreement

between the Skyrme and lattice results to occur near the chiral limit, where the isovector contribution becomes dominant.

The dependence of the spatial distribution of the pseudoscalar correlation function on the quark mass is shown in Figure 5. Although in principle one has the same competition between the shrinking scale parameter and growing pion tail as in the density-density correlation function, we observe that the pseudoscalar correlation function has extremely mild mass dependence in the range 0-2 fm. The only qualitative feature which is not shown in this plot is the fact that in the Skyrme model, the volume integral of this correlation function is zero, as it is in any independent particle approximation⁷. Thus, the function has a node and an exterior negative region of equal volume. When the correlation function is plotted at larger distances, one observes that as the pion mass becomes lower, the tail extends to larger distances and the node moves outward.

The comparison of the Skyrme model pseudoscalar correlation functions with the lattice results is shown in Figure 6. On the lattice we observe that the overall size is very different, as expected because of the large isoscalar contribution at the quark masses we have used. However, it is significant that as the pion mass decreases, the lattice result becomes much closer to the Skyrme solution. The outward movement of the node is particularly evident in Figure 6. The stability of the Skyrme correlation function when varying the mass compared to the large change of the lattice result suggests that a significant part of change in the lattice result arises from the diminishing contribution of the isoscalar term. Again it would be very interesting to follow the behavior to lower quark masses. As a technical point, we note that because of the node at large distance and the slow spatial decay at small pion mass, the pseudoscalar correlation function is more sensitive to finite size effects on the lattice, and is more difficult to extrapolate to the physical pion mass than the density-density correlation function.

IV. SUMMARY AND CONCLUSIONS

In this work, we have derived the analytic results necessary to compare the density-density and pseudoscalar correlation functions calculated in lattice QCD with the Skyrme model and taken the first step in using quenched lattice QCD as a laboratory to systematically explore the Skyrme effective field theory. The principal numerical results are presented in Figures 4 and 6. We observe in Figure 4 that already for a quark mass of 40 MeV, corresponding to a pion mass of 340 MeV, the Skyrme approximation to the density-density correlation function appears to be in good agreement with the lattice result. In contrast, because of substantial isoscalar contributions in quenched QCD for a pion mass of 340 MeV, which are excluded by construction from the Skyrme model, the Skyrme pseudoscalar correlation function is not quantitatively correct, although the trend with decreasing pion mass is encouraging.

These exploratory results suggest several promising directions for future research. At the most pedestrian level, it will clearly be worthwhile to extend the comparison to lighter quark masses. More interesting and potentially extremely useful, is the opportunity to use lattice techniques to calculate numerically the effective action and effective operators and thus evaluate corrections to the Skyrme approximation. As described in the introduction, this provides a consistent framework to systematically explore the quantitative effects of

truncation in meson fields, of truncation of the effective action, of truncation of the expansion of effective operators, and of truncation of the quantum loop corrections. Thus, rather than using the lattice to calculate hadron observables directly, one can instead use it to calculate from first principles the relevant parameters of an effective theory which could then be applied much more generally than one could hope to apply the full apparatus of lattice QCD.

Acknowledgments

It is a pleasure to acknowledge illuminating discussions with Suzhou Huang and Janos Polonyi. The authors also gratefully acknowledge the hospitality of the Institute for Nuclear Theory, where this work and manuscript were completed, and the supercomputer resources for the lattice calculations provided by the National Energy Research Supercomputer Center.

REFERENCES

1. T. H. R. Skyrme, *Proc. Roy. Soc.* **A260** (1961) 127.
2. G. S. Adkins, C. R. Nappi and E. Witten, *Nucl. Phys.* **B228** (1983) 552.
3. G. S. Adkins and C. R. Nappi, *Nucl. Phys.* **B233** (1984) 109.
4. I. Zahed and G. E. Brown, *Physics Reports* **142** (1986) 1.
5. S. Huang, *Nucl. Phys.* **B324** (1989) 34.
6. J. Goldstone and F. Wilczek, *Phys. Rev. Lett.* **47** (1981) 986.
7. M. Lissia, M.-C. Chu, J. W. Negele and J. M. Grandy, *Nucl. Phys.* **A555** (1993) 272.
8. M.-C. Chu, M. Lissia and J. W. Negele, *Nucl. Phys.* **B360** (1991) 31.
9. M.-C. Chu, J. M. Grandy, M. Lissia and J. W. Negele, *Nucl. Phys. B (Proc. Suppl.)* **26** (1992) 412.
10. J. Grandy, Ph. D. Thesis (1992) M.I.T., Cambridge, MA.
11. M. Burkardt, J. M. Grandy, and J. W. Negele, MIT preprint CTP#2109 (1993).
12. P. Bacilieri *et. al.*, *Nucl. Phys.* **B317** (1989) 509.

APPENDIX

In this Appendix we review the main features of the Skyrme model, we give an explicit derivation of the time component of the vector current without averaging over angular variables (which is also useful for other applications) and we perform the angular integration when the two currents are kept at fixed relative distance. As in the rest of the paper we have tried to keep notation consistent with Refs. [2,3], from which Eqs. (A.1) through (A.7) are taken.

The Lagrangian of the model is (Ref. [3])

$$\mathcal{L} = \frac{1}{16} F_\pi^2 \text{tr} [\partial_\mu U \partial^\mu U^\dagger] + \frac{1}{32e^2} \text{tr} \left[[(\partial_\mu U) U^\dagger, (\partial_\mu U) U^\dagger]^2 \right] + \frac{1}{8} m_\pi^2 F_\pi^2 (\text{tr} U - 2) \quad . \quad (\text{A.1})$$

If we substitute the spinning hedgehog *ansatz*

$$\begin{aligned} U &= A(t) U_0(\vec{r}) A^\dagger(t) \quad , \quad A(t) \in SU(2) \\ U_0(\vec{r}) &= e^{iF(\vec{r})\vec{\tau}\cdot\hat{r}} \end{aligned} \quad (\text{A.2a})$$

into (A.1), we obtain after quantization the following expression for the energy (Ref. [2]):

$$E = \frac{F_\pi}{e} \left[M + \frac{e^4}{8\tilde{\lambda}} 2J(2J+2) \right] \quad (\text{A.3})$$

where J is the spin (equal to isospin in this model) of the particle

$$M = \int d^3\tilde{r} \left\{ \frac{1}{8} \left[\left(\frac{dF}{d\tilde{r}} \right)^2 + 2 \frac{\sin^2 F}{\tilde{r}^2} \right] + \frac{1}{2} \left[2 \left(\frac{dF}{d\tilde{r}} \right)^2 + \frac{\sin^2 F}{\tilde{r}^2} \right] \frac{\sin^2 F}{\tilde{r}^2} + \frac{1}{4} \beta^2 (1 - \cos F) \right\} \quad , \quad (\text{A.4})$$

$\tilde{\lambda}$ was defined in Eq. (2.6c), $\tilde{r} = eF_\pi r$ and $\beta = \frac{m_\pi}{eF_\pi}$. $F(\tilde{r})$ is chosen so that it minimizes M with the boundary conditions $F(0) = \pi$ and $F(\infty) = 0$ to ensure that the baryon number (integral of Eq. (2.5)) is equal to 1; the resulting equation for $F(\tilde{r})$ is

$$\begin{aligned} \left(\frac{1}{4} \tilde{r}^2 + 2 \sin^2 F \right) \frac{d^2 F}{d\tilde{r}^2} + 2 \sin F \cos F \left(\frac{dF}{d\tilde{r}} \right)^2 + \frac{1}{2} \tilde{r} \frac{dF}{d\tilde{r}} \\ - 2 \sin F \cos F \left(\frac{1}{4} + \frac{\sin^2 F}{\tilde{r}^2} \right) - \frac{1}{4} \beta^2 \tilde{r}^2 \sin F = 0 \quad . \end{aligned} \quad (\text{A.5})$$

The general form of the time component of the Noether current associated with the $V - A$ transformation $\delta U = i\tau_a U$ of the Lagrangian (A.1) is (Ref. [2]):

$$\begin{aligned} J_{V-A}^{0,a} &= \frac{1}{8} i F_\pi^2 \text{tr} \{ (\partial^0 U) U^\dagger \tau_a \} + \frac{i}{8e^2} \text{tr} \{ [(\partial_\nu U) U^\dagger, \tau_a] [(\partial^0 U) U^\dagger, (\partial^\nu U) U^\dagger] \} \\ &= \frac{1}{8} i F_\pi^2 \text{tr} \{ (\partial^0 U) U^\dagger \tau_a \} - \frac{i}{8e^2} \Sigma_i \text{tr} \{ [(\partial_i U) U^\dagger, \tau_a] [(\partial^0 U) U^\dagger, (\partial_i U) U^\dagger] \} \quad . \end{aligned} \quad (\text{A.6})$$

By using $\text{Tr} \{ [A, B][C, D] \} = 2 \text{Tr} \{ AD \} \text{Tr} \{ BC \} - 2 \text{Tr} \{ AC \} \text{Tr} \{ BD \}$, valid for A, B, C, D belonging to the $SU(2)$ Lie algebra and the fact that $\partial_\mu U^\dagger = \partial_\mu U^{-1} = -U^{-1} (\partial_\mu U) U^{-1} = -U^\dagger (\partial_\mu U) U^\dagger$, we may rewrite (A.6) as

$$\begin{aligned}
J_{V-A}^{0,a} &= \frac{iF_\pi^2}{8} \text{tr} \{ (\partial^0 U) U^\dagger \tau_a \} - \frac{i}{4e^2} \text{tr} \{ (\partial^0 U) U^\dagger \tau_a \} \Sigma_i \text{tr} \{ [(\partial_i U) U^\dagger]^2 \} \\
&\quad + \frac{i}{4e^2} \Sigma_i \text{tr} \{ (\partial_i U) U^\dagger \tau_a \} \text{tr} \{ (\partial_i U) U^\dagger (\partial_0 U) U^\dagger \} \\
&= \frac{iF_\pi^2}{8} \text{tr} \{ (\partial_0 U) U^\dagger \tau_a \} + \frac{i}{4e^2} \text{tr} \{ (\partial^0 U) U^\dagger \tau_a \} \Sigma_i \text{tr} \{ (\partial_i U) (\partial_i U^\dagger) \} \\
&\quad - \frac{i}{4e^2} \Sigma_i \text{tr} \{ (\partial_i U) U^\dagger \tau_a \} \text{tr} \{ (\partial_i U) (\partial_0 U^\dagger) \} \quad .
\end{aligned} \tag{A.7}$$

Before calculating the four traces we need, let us derive a few useful formulae. Equation (A.2a) can be written as

$$\begin{aligned}
U_0(\vec{r}) &= \cos F + i\vec{\tau} \cdot \hat{r} \sin F \\
U(\vec{r}, t) &= A(t)U_0A^\dagger(t) = \cos F + i\vec{\tau} \cdot \hat{r}_R \sin F
\end{aligned} \tag{A.2b}$$

where \vec{r}_R is the vector \vec{r} rotated according to the law $\vec{r}_R \cdot \vec{\tau} = A\vec{r} \cdot \vec{\tau}A^\dagger$. Using the fact that A is unitary, we obtain

$$\frac{dU}{dt} = \dot{U} = \dot{A}U_0A^\dagger + AU_0\dot{A}^\dagger = \dot{A}A^\dagger AU_0A^\dagger - AU_0A^\dagger \dot{A}A^\dagger = [\dot{A}A^\dagger, U] \quad . \tag{A.8}$$

The spatial derivatives are

$$\begin{aligned}
\frac{\partial U_0}{\partial x_i} &= \partial_i U_0 = \hat{r}_i \frac{dF}{dr} (-\sin F + i \cos F \hat{r} \cdot \vec{\tau}) + i \frac{\sin F}{r} (\tau_i - \hat{r}_i \hat{r} \cdot \vec{\tau}) \\
\frac{\partial U}{\partial x_R^i} &= \partial_i^R U = \hat{r}_{Ri} \frac{dF}{dr} (-\sin F + i \cos F \hat{r}_R \cdot \vec{\tau}) + i \frac{\sin F}{r} (\tau_i - \hat{r}_{Ri} \hat{r}_R \cdot \vec{\tau}) \quad .
\end{aligned} \tag{A.9}$$

We also need to show that

$$\Sigma_i [\partial_i(\dots)] [\partial_i(\dots)] = \Sigma_i [\partial_i^R(\dots)] \partial_i^R(\dots) \tag{A.10a}$$

or equivalently that

$$J_{jk} \equiv \Sigma_i \frac{\partial r_{Rj}}{\partial r_i} \frac{\partial r_{Rk}}{\partial r_i} = \delta_{jk} \quad . \tag{A.10b}$$

This is because it is more convenient to take derivatives of U with respect to \vec{r}_R (see Eq. (A.9)). Since

$$\frac{\partial r_{Rj}}{\partial r_i} = \frac{\partial}{\partial r_i} \frac{1}{2} \text{tr} \{ \vec{r}_R \cdot \vec{\tau} \tau_j \} = \frac{\partial}{\partial r_i} \frac{1}{2} \text{tr} \{ \vec{r} \cdot \vec{\tau} A^\dagger \tau_j A \} = \frac{1}{2} \text{tr} (\tau_i A^\dagger \tau_j A) \quad .$$

we may write

$$\begin{aligned}
J_{jk} &= \frac{1}{4} \Sigma_i \text{tr} \{ \tau_i (A^\dagger \tau_j A) \} \text{tr} \{ \tau_i (A^\dagger \tau_k A) \} \\
&= \Sigma_i \frac{1}{2} \{ (A^\dagger \tau_j A) (A^\dagger \tau_k A) \} = \frac{1}{2} \text{tr} \{ \tau_j \tau_k \} = \delta_{jk} \quad ,
\end{aligned} \tag{A.10c}$$

where we used the fact that

$$\frac{1}{2} \text{tr} \{M_1 M_2\} = \frac{1}{2} \text{tr} \{M_1\} \frac{1}{2} \text{tr} \{M_2\} + \Sigma_i \frac{1}{2} \text{tr} \{\tau_i M_1\} \frac{1}{2} \text{tr} \{\tau_i M_2\} \quad , \quad M_1, M_2 \in SU(2) \quad . \quad (\text{A.11})$$

This is the component form of the scalar product in $SU(2)$. Now we are ready to calculate the traces in Eq. (A.7). The first one gives

$$\begin{aligned} \text{tr} \{(\partial_0 U) U^\dagger \tau_a\} &= \text{tr} \left\{ \left[\dot{A} A^\dagger, U \right] U^\dagger \tau_a \right\} \\ &= \text{tr} \left\{ \left[\dot{A} A^\dagger, i \sin F \hat{r}_R \cdot \vec{\tau} \right] (\cos F - i \sin F \hat{r}_R \cdot \vec{\tau}) \tau_a \right\} \\ &= i \sin F \cos F \text{tr} \left\{ \left[\dot{A} A^\dagger, \hat{r}_R \cdot \vec{\tau} \right] \tau_a \right\} + \sin^2 F \text{tr} \left\{ \left[\dot{A} A^\dagger, \hat{r}_R \cdot \vec{\tau} \right] \hat{r}_R \cdot \vec{\tau} \tau_a \right\} \\ &= i \sin(2F) \text{tr} \left\{ \dot{A} A^\dagger \hat{r}_R \cdot \vec{\tau} \tau_a \right\} + 2 \sin^2 F \text{tr} \left\{ \dot{A} A^\dagger \tau_a \right\} \\ &\quad - \sin^2 F \text{tr} \left\{ \dot{A} A^\dagger \hat{r}_R \cdot \vec{\tau} \right\} \text{tr} \left\{ \hat{r}_R \cdot \vec{\tau} \tau_a \right\} \quad , \end{aligned} \quad (\text{A.12})$$

where we used $\text{tr} \{[A, B]CD\} = \text{tr} \{AD\} \text{tr} \{BC\} - \text{tr} \{AC\} \text{tr} \{BD\}$ and $\text{tr} \{ABC\} = -\text{tr} \{BAC\}$ for A, B, C, D , belonging to the $SU(2)$ Lie algebra to go from the second last to the last line. The second trace is

$$\begin{aligned} \Sigma_i \text{tr} \{(\partial_i U) (\partial_i U^\dagger)\} &= \Sigma_i \text{tr} \left\{ (\partial_i U_0) (\partial_i U_0^\dagger) \right\} \\ &= \Sigma_i \text{tr} \left\{ \left[\hat{r}_i \frac{dF}{dr} (-\sin F + i \cos F \hat{r} \cdot \vec{\tau}) + i \frac{\sin F}{r} (\tau_i - \hat{r}_i \hat{r} \cdot \vec{\tau}) \right] \right. \\ &\quad \left. \times \left[\hat{r}_i \frac{dF}{dr} (-\sin F - i \cos F \hat{r} \cdot \vec{\tau}) - i \frac{\sin F}{r} (\tau_i - \hat{r}_i \hat{r} \cdot \vec{\tau}) \right] \right\} \\ &= \text{tr} \left\{ \left(\frac{dF}{dr} \right)^2 + \frac{\sin^2 F}{r^2} (\vec{\tau}^2 - 2 + 1) \right\} = 2 \left[\left(\frac{dF}{dr} \right)^2 + 2 \frac{\sin^2 F}{r^2} \right] \quad . \end{aligned} \quad (\text{A.13})$$

The third trace is, using the fact that in the last term of Eq. (A.7) we shall take advantage of property (A.10a) to change ∂_i into ∂_i^R ,

$$\begin{aligned} \text{tr} \{(\partial_i^R U) U^\dagger \tau_a\} &= \text{tr} \left\{ \left[\hat{r}_{Ri} \frac{dF}{dr} (-\sin F + i \cos F \hat{r}_R \cdot \vec{\tau}) + i \frac{\sin F}{r} (\tau_i - \hat{r}_{Ri} \hat{r}_R \cdot \vec{\tau}) \right] \right. \\ &\quad \left. \times [\cos F - i \sin F \hat{r}_R \cdot \vec{\tau}] \tau_a \right\} \\ &= \hat{r}_{Ri} \text{tr} \{ \dots \} + i \frac{\sin F}{r} \text{Tr} \{ [\cos F - i \sin F \hat{r}_R \cdot \vec{\tau}] \tau_a \tau_i \} \quad . \end{aligned} \quad (\text{A.14})$$

We do not write out the term proportional to \hat{r}_{Ri} , because it will not contribute when multi-

plied times the fourth trace, which is

$$\begin{aligned}
\text{tr} \{(\partial_0 U) (\partial_i^R U^\dagger)\} &= \text{tr} \left\{ \left[\dot{A} A^{-1}, U \right] \partial_i^R U^{-1} \right\} = \text{tr} \left\{ \dot{A} A^{-1} [U, \partial_i^R U^{-1}] \right\} \\
&= \text{tr} \left\{ \dot{A} A^{-1} \left[i \sin F \hat{r}_R \cdot \vec{\tau}, -i \frac{\sin F}{r} \tau_i \right] \right\} \\
&= \frac{\sin^2 F}{r} \text{tr} \left\{ \dot{A} A^{-1} [\hat{r}_R \cdot \vec{\tau}, \tau_i] \right\} = 2 \frac{\sin^2 F}{r} \text{tr} \left\{ \dot{A} A^{-1} \hat{r}_R \cdot \vec{\tau} \tau_i \right\} .
\end{aligned} \tag{A.15}$$

Now we multiply Eq. (A.14) times Eq. (A.15) and sum over i to get the last term of Eq. (A.7). Note that the first term in Eq. (A.14) when multiplied times Eq. (A.15) gives a result proportional to $\text{tr} \left\{ \dot{A} A^{-1} (\hat{r}_R \cdot \vec{\tau})^2 \right\} = \text{tr} \left\{ \dot{A} A^{-1} \right\} = 0$. To combine the trace in the second term with the one in Eq. (A.15) we may use Eq. (A.11):

$$\begin{aligned}
&\Sigma_i \text{tr} \{(\partial_i U) U^\dagger \tau_a\} \text{tr} \{(\partial_i U) (\partial_0 U^\dagger)\} \\
&= \Sigma_i \text{tr} \{(\partial_i^R U) U^\dagger \tau_a\} \text{tr} \{(\partial_i^R U) (\partial_0 U^\dagger)\} \\
&= i 8 \frac{\sin^3 F}{r^2} \frac{1}{2} \text{tr} \left\{ \dot{A} A^\dagger \hat{r}_R \cdot \vec{\tau} \tau_i \right\} \frac{1}{2} \text{tr} \{[\cos F - i \sin F \hat{r}_R \cdot \vec{\tau}] \tau_a \tau_i\} \\
&= i 8 \frac{\sin^3 F}{r^2} \left(\frac{1}{2} \text{tr} \left\{ \dot{A} A^\dagger \hat{r}_R \cdot \vec{\tau} [\cos F - i \sin F \hat{r}_R \cdot \vec{\tau}] \tau_a \right\} \right. \\
&\quad \left. - \frac{1}{2} \text{tr} \left\{ \dot{A} A^\dagger \hat{r}_R \cdot \vec{\tau} \right\} \frac{1}{2} \text{tr} \{-i \sin F \hat{r}_R \cdot \vec{\tau} \tau_a\} \right) \\
&= 2 \frac{\sin^2 F}{r^2} \left[i \sin 2F \text{tr} \left\{ \dot{A} A^\dagger \hat{r}_R \cdot \vec{\tau} \tau_a \right\} + 2 \sin^2 F \text{tr} \left\{ \dot{A} A^\dagger \tau_a \right\} \right. \\
&\quad \left. - \sin^2 F \text{tr} \left\{ \dot{A} A^\dagger \hat{r}_R \cdot \vec{\tau} \right\} \text{tr} \left\{ \hat{r}_R \cdot \vec{\tau} \tau_a \right\} \right] .
\end{aligned} \tag{A.16}$$

The expression in brackets is equal to $\text{tr} \{(\partial_0 U) U^\dagger \tau_a\}$ (Eq. (A.12)), which appears in both the other two terms in Eq. (A.7). We then insert Eq. (A.12), Eq. (A.13) and Eq. (A.14) into Eq. (A.7) and obtain

$$\begin{aligned}
J_{V-A}^{0,a} &= \frac{iF^2}{4} \left[\sin^2 F \text{tr} \left\{ \dot{A} A^\dagger \tau_a \right\} + \frac{i}{2} \sin 2F \text{tr} \left\{ \dot{A} A^\dagger \hat{r}_R \cdot \vec{\tau} \tau_a \right\} - \hat{r}_{Ra} \sin^2 F \text{tr} \left\{ \dot{A} A^\dagger \hat{r}_R \cdot \vec{\tau} \right\} \right] \\
&\quad \times \left[1 + \frac{4}{(eF\pi)^2} \left(\left(\frac{dF}{dr} \right)^2 + \frac{\sin^2 F}{r^2} \right) \right] .
\end{aligned} \tag{A.17}$$

As in Ref. [2], one can convince oneself that $J_{V+A}^{0,a}$ is obtained from Eq. (A.7) by exchanging $U \leftrightarrow U^{-1}$, *i.e.* $\hat{r}_R \leftrightarrow -\hat{r}_R$. Then J_V will contain terms even in \hat{r}_R and J_A terms odd in \hat{r}_R ,

as expected from parity considerations:

$$\begin{aligned}
J_V^{0,a} &= J_{V+A}^{0,a} + J_{V-A}^{0,a} = \frac{iF_\pi^2}{2} \sin^2 F \left[1 + \frac{4}{(eF_\pi)^2} \left(\left(\frac{dF}{dr} \right)^2 + \frac{\sin^2 F}{r^2} \right) \right] \\
&\quad \times \left[\text{tr} \left\{ \dot{A} A^{-1} \tau_a \right\} - \hat{r}_{Ra} \text{tr} \left\{ \dot{A} A^\dagger \hat{r}_R \cdot \vec{\tau} \right\} \right] \\
&= 3iF_\pi^2 \Lambda(\tilde{r}) \left[\text{tr} \left\{ \dot{A} A^{-1} \tau_a \right\} - \hat{r}_{Ra} \text{tr} \left\{ \dot{A} A^\dagger \hat{r}_R \cdot \vec{\tau} \right\} \right] \\
&= F_\pi^2 \frac{\Lambda(\tilde{r})}{\lambda} \left\{ 2I_a - \left[3\vec{I} \cdot \hat{r}_R \hat{r}_{Ra} - I_a \right] \right\} , \tag{A.18}
\end{aligned}$$

where we used the definitions of Λ and λ , Eqs. (2.6b) and (2.6c). We also used the fact that $\dot{A} A^{-1} = -\frac{i}{2\lambda} \vec{I} \cdot \vec{\tau}$ with \vec{I} the isospin operator, as may be derived from $A = a_0 + i\vec{a} \cdot \vec{\tau}$, $\vec{\pi} = 4\lambda\vec{a}$ and $\vec{I} = -\frac{1}{2} [a_0 \vec{\pi} - \vec{a} \pi_0 - \vec{a} \times \vec{\pi}]$ which can be found in Ref. [2]. For completeness, the time component of the axial current is

$$J_A^{0,a} = J_{V+A}^{0,a} - J_{V-A}^{0,a} = \frac{F_\pi^2}{4\lambda} \sin 2F \left\{ 1 + \frac{4}{(eF_\pi)^2} \left[\left(\frac{dF}{dr} \right)^2 + \frac{\sin^2 F}{r^2} \right] \right\} \left(\vec{I} \times \hat{r}_R \right)_a , \tag{A.19}$$

in agreement with Ref. [3].

We calculate only the correlations between currents in proton (or neutron), $\langle N|VV|N \rangle$, and not off-diagonal matrix elements, $\langle N|VV|N' \rangle$. Hence, we only need:

$$\begin{aligned}
\text{diag} \left[J_V^{0,3}(\vec{r}) J_V^{0,3}(\vec{r}') \right] &= F_\pi^4 \frac{9\Lambda(\tilde{r})\Lambda(\tilde{r}')}{\lambda^2} \text{diag} \left[(I_3 - \vec{I} \cdot \hat{r}_3) (I_3 - \vec{I} \cdot \hat{r}'_3) \right] \\
&= F_\pi^4 \frac{9\Lambda(\tilde{r})\Lambda(\tilde{r}')}{\lambda^2} \left\{ (I_3)^2 - \hat{r}_i \hat{r}_3 \text{diag} (I_i I_3) - \hat{r}'_i \hat{r}'_3 \text{diag} (I_i I_3) + \hat{r}_i \hat{r}_3 \hat{r}'_j \hat{r}'_j \text{diag} (I_i I_j) \right\} \\
&= F_\pi^4 \frac{9\Lambda(\tilde{r})\Lambda(\tilde{r}')}{\lambda^2} (I_3)^2 \left\{ 1 - \cos^2 \theta - \cos^2 \theta' + \cos \gamma \cos \theta \cos \theta' \right\} , \tag{A.20}
\end{aligned}$$

where γ is the angle between \vec{r} and \vec{r}' .

The correlation we want is then (note that we changed variables of integration from \vec{r}, \vec{r}' to \vec{r}_R, \vec{r}'_R and that $(I_3)^2 = \frac{1}{4}$ both in the proton and neutron):

$$\begin{aligned}
V(y) &= \int \frac{d\vec{r} d\vec{r}' \delta(y - |\vec{r} - \vec{r}'|)}{4\pi y^2} \text{diag} \left[J_V^{0,3}(\vec{r}) J_V^{0,3}(\vec{r}') \right] \\
&= \frac{9}{4} \frac{1}{4\pi y^2} \frac{1}{(e^3 F_\pi \lambda)^2} \int_0^\infty d\tilde{r} \tilde{r}^2 \int_0^\infty d\tilde{r}' \tilde{r}'^2 \Lambda(\tilde{r}) \Lambda(\tilde{r}') \int d\phi \int d\phi' \\
&\quad \times \int d(\cos \theta) \int d(\cos \theta') \delta(y - |\vec{r} - \vec{r}'|) \left[1 - \cos^2 \theta - \cos^2 \theta' + \cos \gamma \cos \theta \cos \theta' \right] \tag{A.21}
\end{aligned}$$

Now we use

$$\delta(y - |\vec{r} - \vec{r}'|) = 2y \delta(y^2 - (\vec{r} - \vec{r}')^2) = \frac{\tilde{y} e F_\pi}{\tilde{r} \tilde{r}'} \delta \left(\cos \gamma - \frac{\tilde{r}^2 + \tilde{r}'^2 - \tilde{y}^2}{2\tilde{r} \tilde{r}'} \right) , \tag{A.22}$$

where $\tilde{y} = eF_\pi$; we change variables from $\phi, \theta, \phi', \theta'$ to $\phi, \theta, \Phi, \gamma$, where Φ and γ are the angles of \vec{r}' with respect to \vec{r} (the transformation is just a rotation and its Jacobian is one); and we use the following identities

$$\cos \theta' = \cos \theta \cos \gamma \pm \sin \theta \sin \gamma \cos(\phi \pm \Phi) \quad , \quad (\text{A.23a})$$

$$\int d\phi \cos \theta' = 2\pi \cos \theta \cos \gamma \quad , \quad (\text{A.23b})$$

$$\int d\phi \cos^2 \theta' = 2\pi \left[\cos^2 \theta \cos^2 \gamma + \frac{1}{2} \sin^2 \theta \sin^2 \gamma \right] \quad , \quad (\text{A.23c})$$

Note that we need only (A.23b) and (A.23c) that can be derived from (A.23a) without knowing the signs which depend on conventions. Then,

$$\begin{aligned} V(y) &= \frac{9}{4} \frac{1}{(e^3 F_\pi \lambda)^2} \frac{(eF_\pi)^3}{4\pi\tilde{y}} \int_0^\infty d\tilde{r} \tilde{r} \Lambda(\tilde{r}) \int_0^\infty d\tilde{r}' \tilde{r}' \Lambda(\tilde{r}') (2\pi)^2 \int d(\cos \theta) \int d(\cos \gamma) \\ &\quad \times \delta \left(\cos \gamma - \frac{\tilde{r}^2 + \tilde{r}'^2 - \tilde{y}^2}{2\tilde{r}\tilde{r}'} \right) \\ &\quad \times \left[1 - \cos^2 \theta - \cos^2 \theta \cos^2 \gamma - \frac{1}{2} (1 - \cos^2 \theta)(1 - \cos^2 \gamma) + \cos^2 \theta \cos^2 \gamma \right] \\ &= \frac{9\pi}{4} \frac{1}{(e^3 F_\pi \lambda)^2} \frac{(eF_\pi)^3}{\tilde{y}} \int_0^\infty d\tilde{r} \tilde{r} \Lambda(\tilde{r}) \int_0^\infty d\tilde{r}' \tilde{r}' \Lambda(\tilde{r}') \\ &\quad \times \int_{-1}^1 dz \delta \left(z - \frac{\tilde{r}^2 + \tilde{r}'^2 - \tilde{y}^2}{2\tilde{r}\tilde{r}'} \right) \frac{1}{2} (1 + z^2) \int_{-1}^1 dx (1 - x^2) \\ &= \frac{3\pi}{2} \frac{(eF_\pi)^3}{\tilde{y}} \frac{1}{(e^3 F_\pi \lambda)^2} \int_0^\infty d\tilde{r} \tilde{r} \Lambda(\tilde{r}) \int_0^\infty d\tilde{r}' \tilde{r}' \Lambda(\tilde{r}') \\ &\quad \times \left[1 + \left(\frac{\tilde{r}^2 + \tilde{r}'^2 - \tilde{y}^2}{2\tilde{r}\tilde{r}'} \right)^2 \right] \theta (2\tilde{r}\tilde{r}' - |\tilde{r}^2 + \tilde{r}'^2 - \tilde{y}^2|) \\ &= 3\pi \frac{(eF_\pi)^3}{\tilde{y}} \frac{1}{(e^3 F_\pi \lambda)^2} \int_{\frac{1}{2}\tilde{y}}^\infty d\tilde{r} \tilde{r} \Lambda(\tilde{r}) \int_{|\tilde{r}-\tilde{y}|}^{\tilde{r}} d\tilde{r}' \tilde{r}' \Lambda(\tilde{r}') \left[1 + \left(\frac{\tilde{r}^2 + \tilde{r}'^2 - \tilde{y}^2}{2\tilde{r}\tilde{r}'} \right)^2 \right] \quad , \end{aligned} \quad (\text{A.24})$$

where in the last line we use the fact that the integrand is symmetric in \tilde{r} and \tilde{r}' to impose $\tilde{r} \geq \tilde{r}'$ and multiply the result times two; with this condition $2\tilde{r}\tilde{r}' \geq |\tilde{r}^2 + \tilde{r}'^2 - \tilde{y}^2| \Leftrightarrow \tilde{r}' \geq |\tilde{r} - \tilde{y}|$ which in turn implies $\tilde{r} > \frac{1}{2}\tilde{y}$. The other two angular integrals we need can be derived in the same way:

$$\int \frac{d\vec{r} d\vec{r}'}{4\pi y^2} \delta(y - |\vec{r} - \vec{r}'|) F(r) F(r') = \frac{4\pi}{y} \int_{\frac{1}{2}y}^\infty dr r F(r) \int_{|y-r|}^r dr' r' F(r') \quad (\text{A.25})$$

and

$$\begin{aligned} &\int \frac{d\vec{r} d\vec{r}'}{4\pi y^2} \delta(y - |\vec{r} - \vec{r}'|) F(r) F(r') \cos \theta \cos \theta' \\ &= \frac{1}{3} \int \frac{d\vec{r} d\vec{r}'}{4\pi y^2} \delta(y - |\vec{r} - \vec{r}'|) F(r) F(r') \cos \gamma \\ &= \frac{4\pi}{3y} \int_{\frac{1}{2}y}^\infty dr r F(r) \int_{|y-r|}^r dr' r' F(r') \left(\frac{r^2 + r'^2 - y^2}{2rr'} \right) \quad . \end{aligned} \quad (\text{A.26})$$

Note that the limit for vanishing y of each of the last three equations is finite⁷.

Figure Captions

- Fig. 1 Pseudoscalar correlation function in the Skyrme model for three alternative definitions of the pseudoscalar current. The solid curve denotes the standard current, Eq. (2.11b), induced by the usual choice of the mass term. The dashed and dot-dashed curves show two other alternatives discussed in the text.
- Fig. 2 Relative contribution of isoscalar and isovector contributions to the density-density correlation function in the Skyrme model. Dashed and dotted lines show the isoscalar and isovector contributions respectively at three representative values of the quark mass, and the weighted combination, Eq. (2.2), is shown by the solid curve.
- Fig. 3 Mass dependence of the density-density correlation function in the Skyrme model. The spatial distribution of the correlation function is shown for each of the four sets of parameters in Table I.
- Fig. 4 Comparison of density-density correlation functions on the lattice and in the Skyrme model. The solid curves denote the Skyrme results for the parameters in Table I corresponding to each lattice quark mass. Lattice measurements of the correlation functions are shown by error bars joined by dashed lines to guide the eye, and all correlation functions are normalized to one at the origin.
- Fig. 5 Mass dependence of the pseudoscalar correlation function in the Skyrme model. The four curves show the spatial distribution of the correlation function for each of the four sets of parameters in Table I.
- Fig. 6 Comparison of pseudoscalar correlation functions on the lattice and in the Skyrme model. The solid curves denote the Skyrme results for the parameters in Table I corresponding to each lattice quark mass. Lattice measurements of the correlation functions are shown by error bars joined by dashed lines to guide the eye, and all correlation functions are normalized to one at the origin.

TABLE I							
Skyrme					Lattice		
κ					0.167	0.1639	0.16
m_q (MeV)		40	95	175	40	95	175
m_π (MeV)	137	342	515	694	340(7)	511(5)	691(3)
e	4.83	3.79	3.23	2.73			
F_π (MeV)	108.1	60.32	46.87	34.87			
$(eF_\pi)^{-1}$ (fm)	0.383	0.862	1.321	2.141			
$\beta = m_\pi/(eF_\pi)$	0.262	1.497	3.402	7.290			
m_N (MeV)	939	915	1097	1321	915(6)	1097(11)	1321(10)
m_Δ (MeV)	1232	1091	1223	1403	1091(23)*	1223(11)	1403(10)
r_S (fm)	0.690	0.917	0.970	1.075			
r_V (fm)	1.048	1.088	1.132	1.256			
$\frac{9}{8}r_S - \frac{1}{8}r_V$ (fm)	0.632	0.894	0.947	1.050	1.0(5)	0.79(20)	0.75(15)

Table I. Parameters of the Skyrme model for lattice calculations corresponding to three different bare quark masses and for physical hadrons. The input hadron masses are shown in bold face font and all other quantities are derived from them. The isoscalar and isovector r.m.s. radii are denoted r_S and r_V respectively. The first column uses physical hadron masses and the next three columns use the lattice hadron masses given in the lattice data shown at the right. The lattice data are taken from Refs. [7-10], with the exception of m_Δ at $\kappa = 0.167$ denoted by an * which was taken from Ref. 12. For reference, we have also tabulated the values of the bare quark mass $m_q \equiv \frac{1}{2\kappa} - \frac{1}{2\kappa_c}$ corresponding to the values of the hopping parameter κ for each lattice.

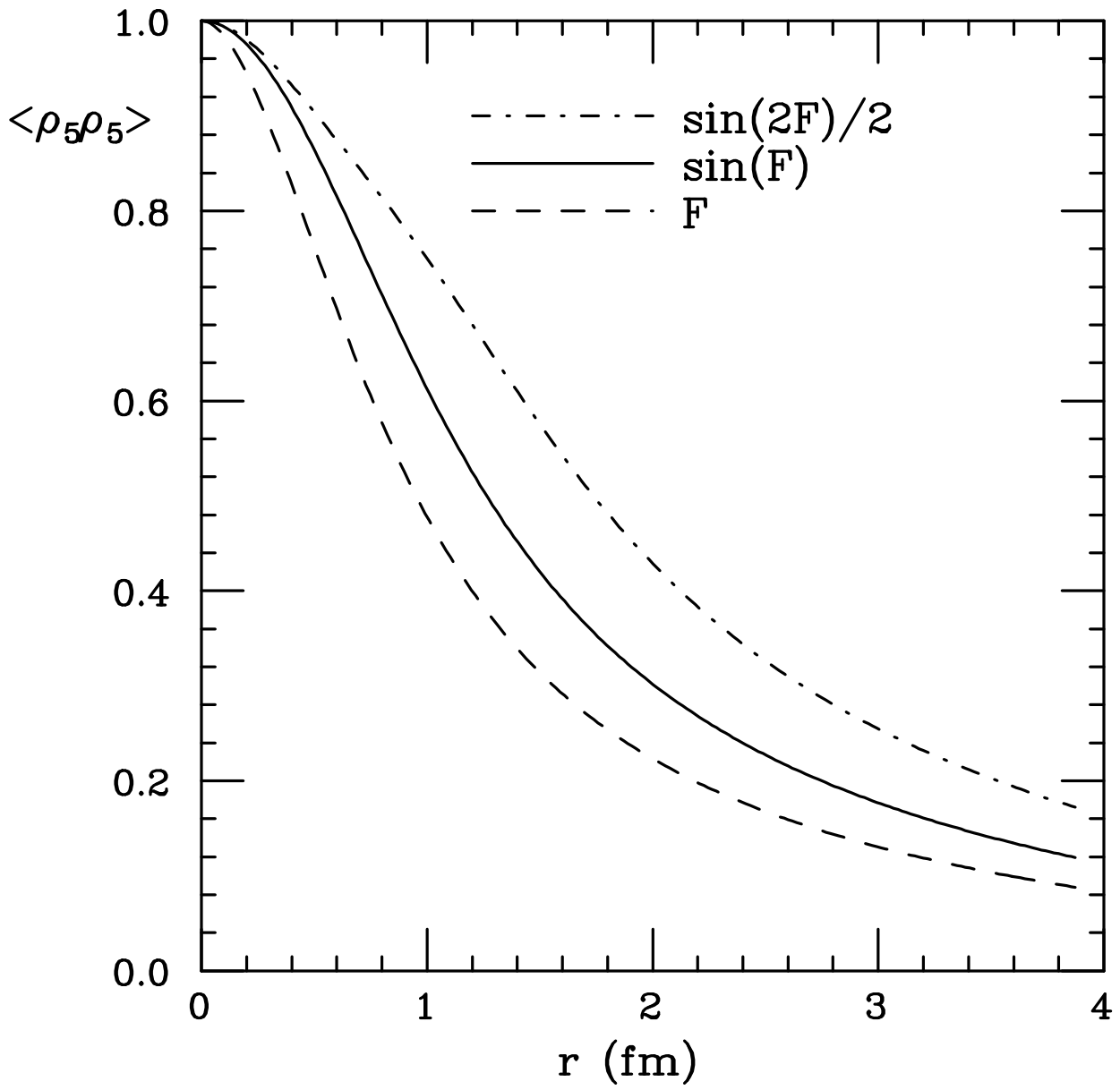


Fig. 1

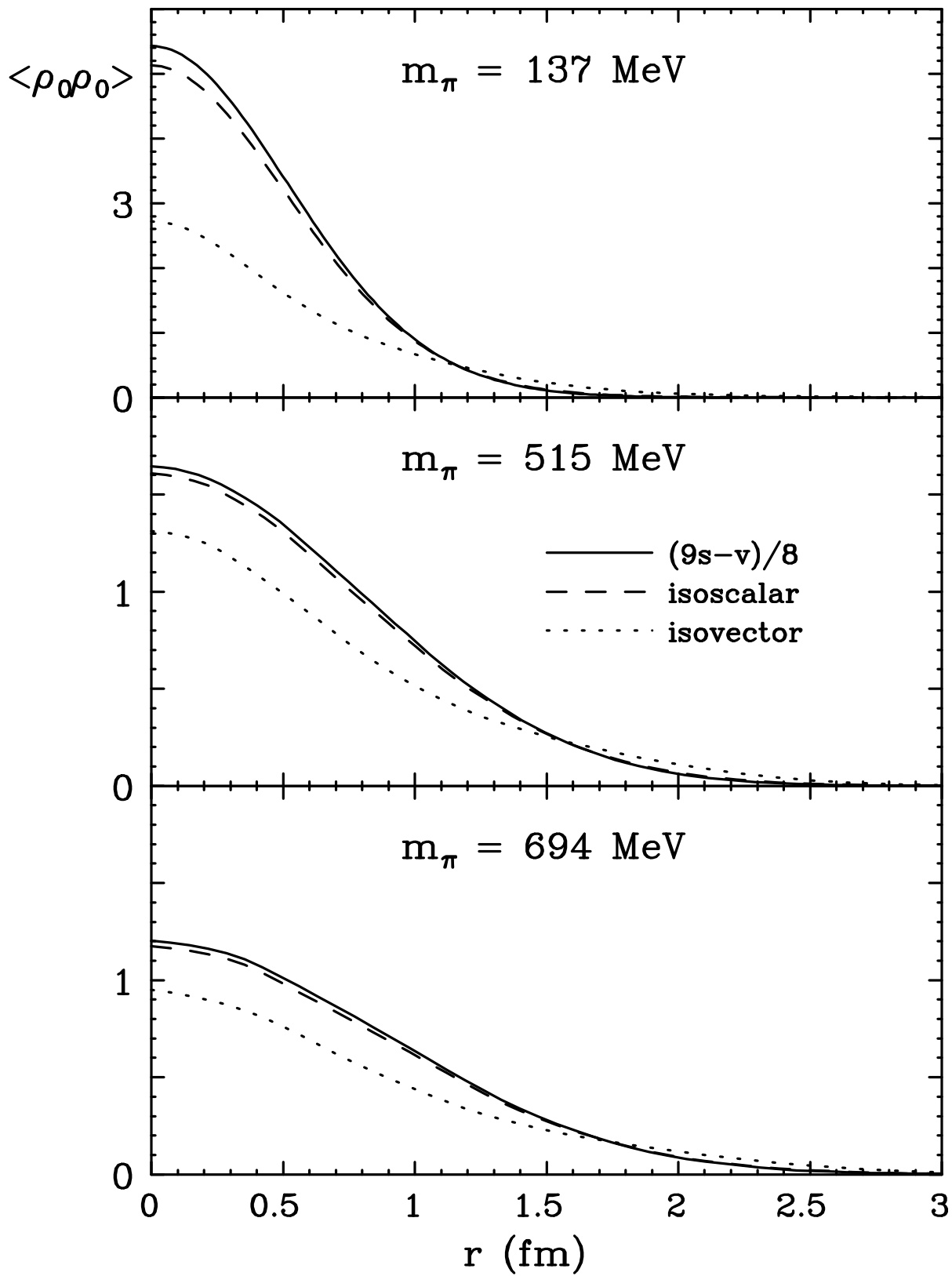


Fig. 2

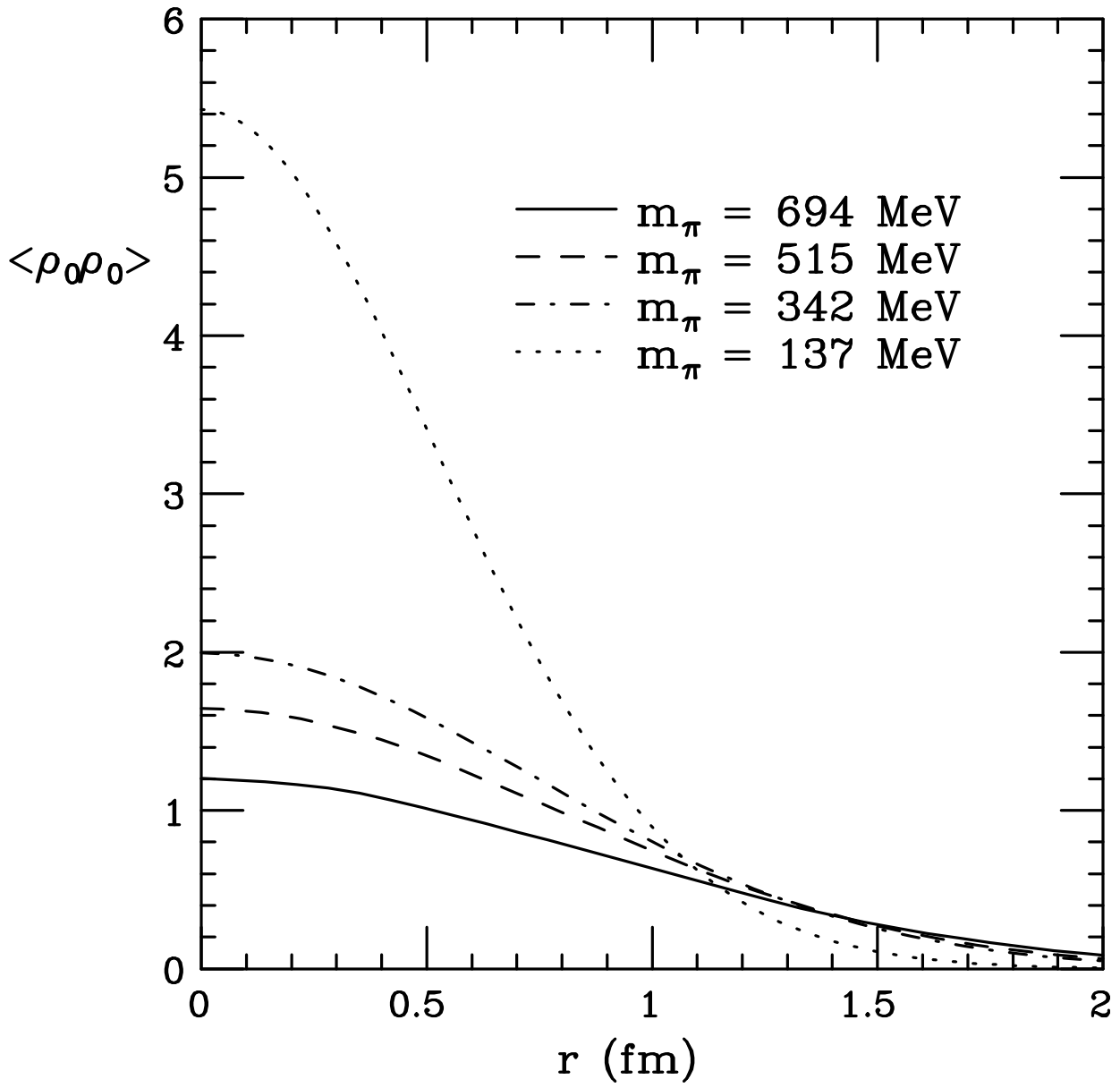


Fig. 3

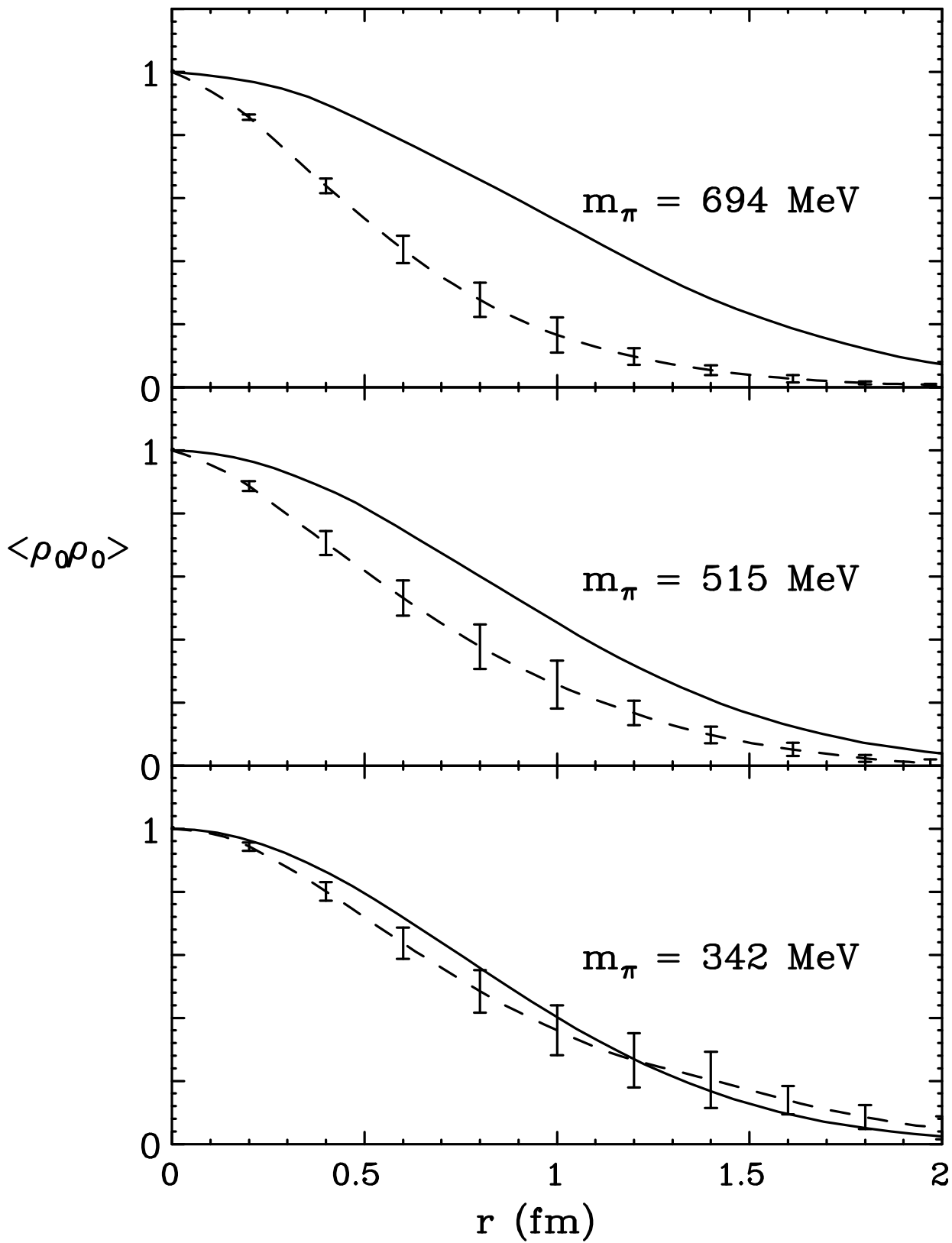


Fig. 4

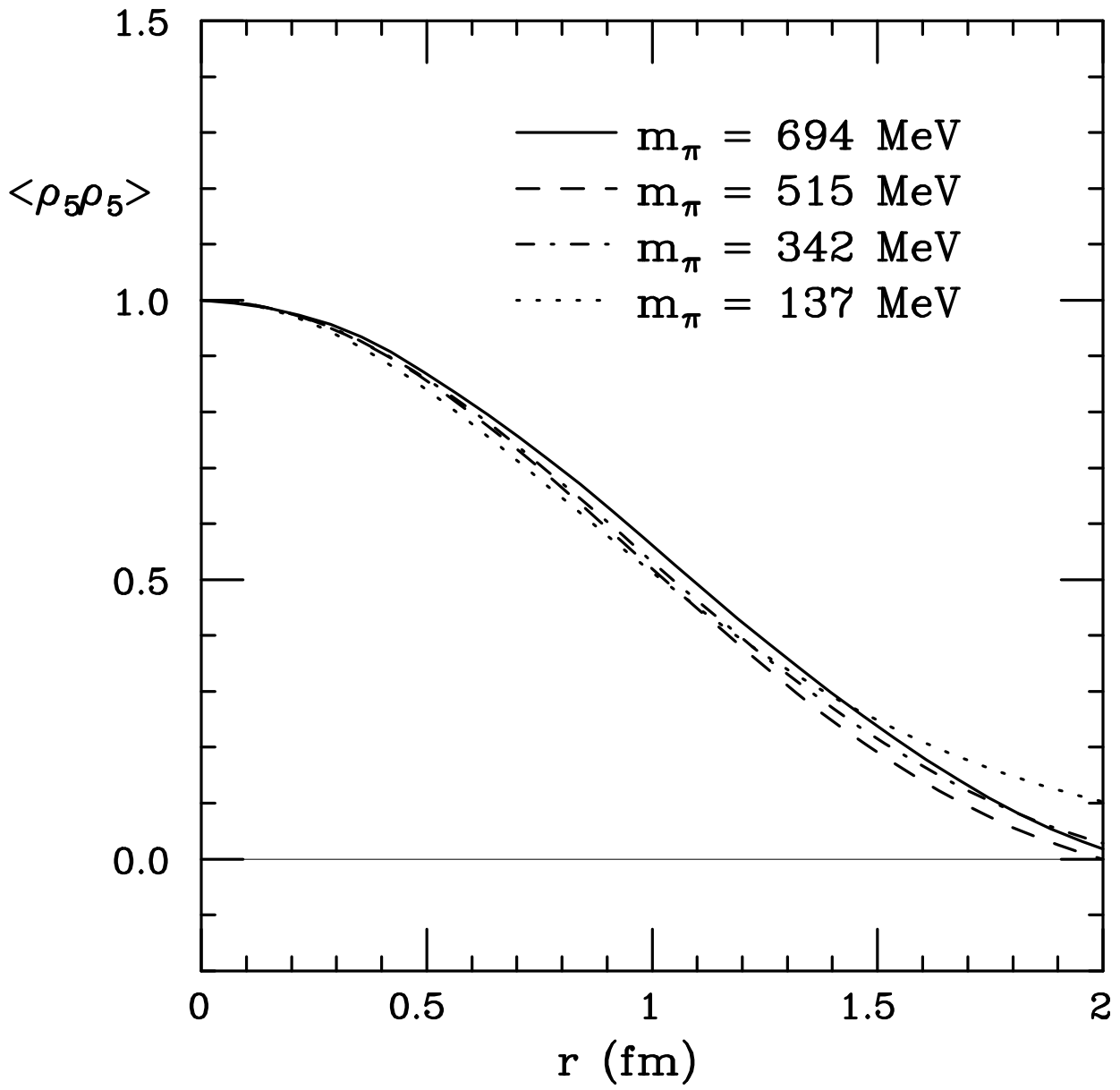


Fig. 5

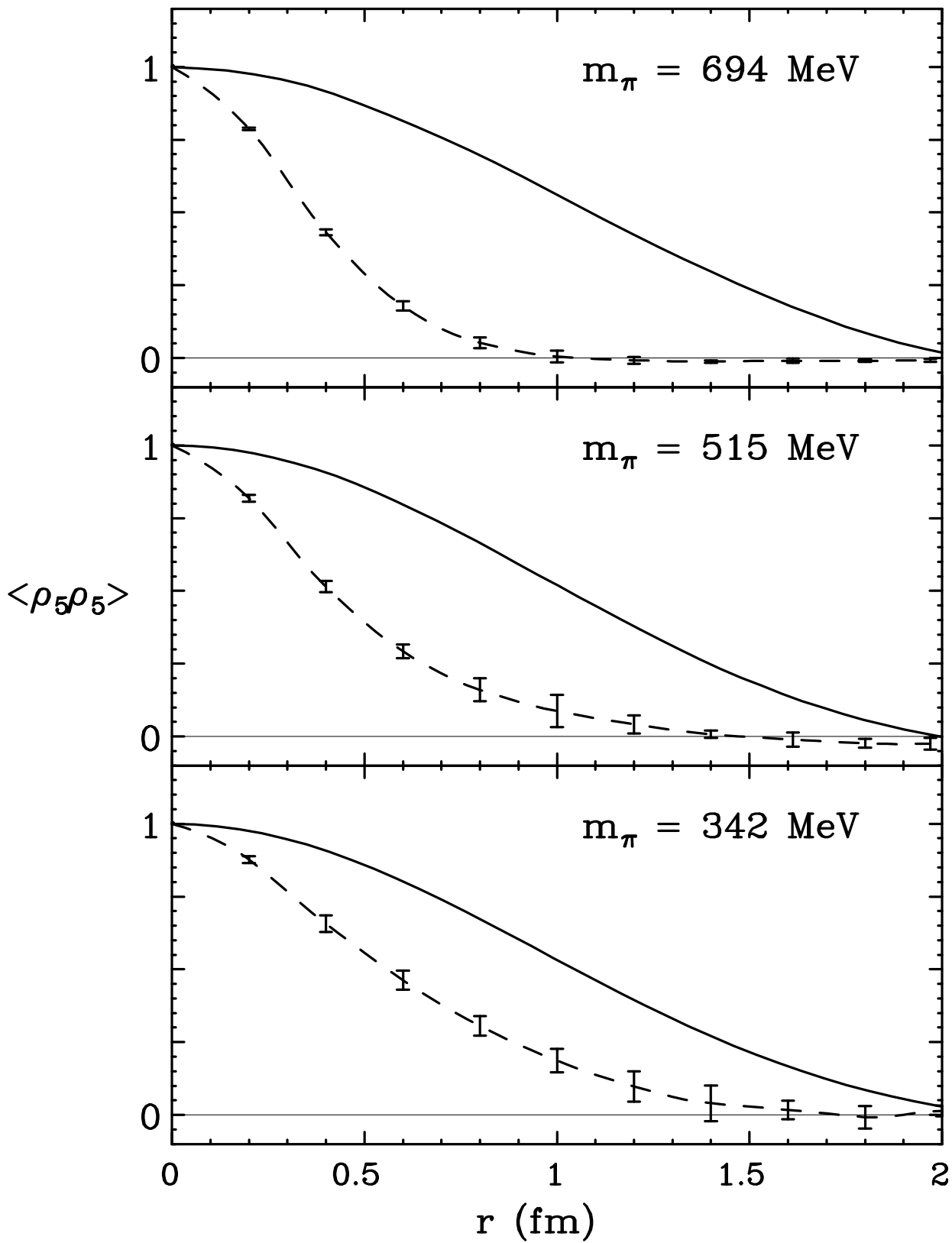


Fig. 6